Absorption and wave packets in optically excited semiconductor superlattices driven by direct-current-alternating-current (dc-ac) fields

2001 J. Phys.: Condens. Matter 13 5103

(http://iopscience.iop.org/0953-8984/13/22/307)

INSTITUTE OF PHYSICS PUBLISHING JOURNAL OF PHYSICS: CONDENSED MATTER

J. Phys.: Condens. Matter **13** (2001) 5103–5113 www.iop.org/Journals/cm PII: S0953-8984(01)21714-7

Absorption and wave packets in optically excited semiconductor superlattices driven by direct-current–alternating-current (dc–ac) fields

W Yan[1], F Claro[1], Z Y Zeng[1] and J Q Liang[2]

[1] Facultad de Física, Pontificia Universidad de Católica de Chile, Casilla 306, Santiago 22, Chile
[2] Institute of Theoretical Physics, Shanxi University, Taiyuan, 030006, People's Republic of China

Received 7 February 2001

Abstract

Within the one-dimensional tight-binding minibands and on-site Coulombic interaction approximation, the absorption spectrum and coherent wave-packet time evolution in an optically excited semiconductor superlattice driven by dc–ac electric fields are investigated using the semiconductor Bloch equations. The dominating roles of the ratios of dc-field Stark to external ac frequency, as well as ac-field Stark to external ac frequency, are emphasized. If the former is an integer $\mathcal{N}$, then also $\mathcal{N}$ harmonics are present within one Stark frequency, while the fractional case leads to the formation of excitonic fractional ladders. The latter ratio determines the size and profile of the wave packet. In the absence of excitonic interaction it controls the maximum size that wave packets reach within one cycle, while the interaction produces a strong anisotropy and tends to palliate the dynamic wave-packet localization.

1. Introduction

The effect of static and/or time-dependent electric fields on superlattices has been the subject of much recent work. Of particular interest is the possibility of terahertz emission caused by Bloch oscillations [1]. The focus in the past has been mainly on the presence of static electric fields, neglecting the THz emission signal propagating in the superlattices. Recently however, in order to interpret the experimental observation of peak shifts in the Wannier–Stark absorption lines of optically excited superlattices, a quasi-static model has been introduced where the THz electric field generated is treated adiabatically [2]. Dignam has shown, however, that this adiabatic treatment of the THz electric field is inadequate [3]. The treatment can be regarded as roughly correct only with the proviso that the interband inverse dephasing time is greater than the THz-field frequency. If this condition is not fulfilled, it is then necessary to treat the static and time-dependent electric fields on an equal footing [3, 4].

It is also known that the combined dc and ac electric fields can induce many interesting and novel phenomena in superlattices. These include the appearance of inverse Bloch oscillators [5, 6], absolute negative conductivity [7], negative absorption (gain) [3], and fractional

Wannier–Stark ladders [8,9]. In this letter we study the absorption and wave-packet dynamics in optically excited semiconductor superlattices under the influence of dc–ac electric fields. It is found that the parameters from both the dc and ac electric fields play important roles in determining their coherent dynamics behaviour. The absorption spectrum is determined by the ratio of the Stark frequency ω_B to the THz-field frequency ω_{ac}. When this ratio is an integer $\mathcal{N}$, $\mathcal{N}$ harmonics appear within the frequency interval ω_B, while if it is a fraction of the form $\omega_B/\omega_{ac} = p/q$, the number of harmonics is q, each being identified as part of the so-called fractional ladder. It is the first time that this fractional structure has been found in the frequency domain by taking into account the excitonic interaction. Also, the effect of the excitonic together with Fano interference on the asymmetric lineshape of the absorption is pointed out. On the other hand, the extent and profile of an electron–hole wave packet is mainly determined by the ratio of the Stark frequency associated with the strength of the THz field, and its frequency. The excitonic interaction produces anisotropy in the wave-packet profile and reduces the dynamic localization effect.

2. Model and numerical results

The coherent dynamics of an optically excited semiconductor superlattice (SL) driven by static and time-dependent electric fields can be described by the following semiconductor Bloch equations [10–12]:

$$\left(\frac{\partial}{\partial t} + \frac{e}{\hbar}\boldsymbol{F}(t)\cdot\boldsymbol{\nabla}_k\right)P_k(t) = -\frac{\mathrm{i}}{\hbar}[e_{e,k} + e_{h,k} - \mathrm{i}\Gamma_L]P_k(t) - \frac{\mathrm{i}}{\hbar}[n_{e,k} + n_{h,k} - 1]\omega_{R,k} \tag{1}$$

$$\left(\frac{\partial}{\partial t} \pm \frac{e}{\hbar}\boldsymbol{F}(t)\cdot\boldsymbol{\nabla}_k\right)n_{e\,(h),k}(t) = -2\,\mathrm{Im}[\omega_{R,k}P_k^*] - \Gamma_T n_{e\,(h),k}(t) \tag{2}$$

where $P_k(t)$ is the interband polarization and $n_{e\,(h),k}(t)$ the electron (hole) population density in the conduction (valence) band. The quantities

$$e_{i,k} = \epsilon_{i,k} - \sum_q V_{|k-q|}n_{i,q} \qquad (i = \mathrm{e}, \mathrm{h})$$

are the renormalized electron and hole energies due to the Coulomb interaction, with $\epsilon_{i,k}$ being the single-particle band energy. Also,

$$\omega_{R,k} = d_{cv}\mathcal{E} + \sum_k V_{|k-q|}P_q$$

are the renormalized Rabi frequencies, with d_{cv} the dipole moment and

$$\mathcal{E}(t) = \mathcal{E}_0\exp(-t^2/\tau^2)\exp(-\mathrm{i}\omega_L t)$$

($\tau = 100$ fs) the Gaussian laser pulse profile. The relaxation time approximation has been assumed, with Γ_L and Γ_T being the longitudinal and transverse relaxation rates, respectively.

We want to obtain the spectrally resolved absorption coefficient and coherent wave-packet dynamics for an optically excited SL driven by the combined dc–ac fields

$$F(t) = F_0 + F_1\cos(\omega_{ac}t).$$

The two components of the electric field are assumed to point along the same direction.

For simplicity, a one-dimensional tight-binding (TB) approximation has been adopted with the two miniband widths and gap energy being Δ_c (conduction), Δ_v (valence), and E_g respectively [4, 11, 13]. This approximation neglects the in-plane continuum contribution to the absorption; the consequences of this are discussed in the following. Firstly, in the

absence of excitonic interaction, the absorption $\alpha(\omega)$ is proportional to the 3D joint density $\rho^{(3)}(\omega)$, which is the convolution product of the one-dimensional joint density of states (JDOS) $\rho^{(1)}(\epsilon)$ and the 2D continuum JDOS $\rho^{(2)}(\epsilon)$ (the latter is a step function changing abruptly at $\epsilon = 0$):

$$\alpha(\omega) \propto \int \rho^{(2)}(\epsilon)\rho^{(1)}(\hbar\omega - \epsilon)\, \mathrm{d}\epsilon.$$

The one-dimensional JDOS $\rho^{(1)}(\epsilon)$ looks like a trapezoid with the concave part in the middle, and it approximately extends over the range $[-\Delta, \Delta]$, where Δ here is the combined miniband width defined as $\Delta = \Delta_c + \Delta_v$. Due to delayed kernel of $\rho^{(1)}(\hbar\omega - \epsilon)$ in the above expression, the resulting $\rho^{(3)}(\omega)$ begins to attain a finite value at $\omega = -\Delta/\hbar$, and becomes approximately constant at $\omega = \Delta/\hbar$ and beyond. That is to say, the behaviour of $\rho^{(2)}(\epsilon)$ at $\epsilon = 0$ changes completely due to the one-dimensional JDOS. Thus, the inclusion of the in-plane continuum contribution can influence the height of characteristic peaks. Because the JDOS is always positive, it cannot turn the gain-type lineshape to a resonance-type shape or vice versa. Secondly, the contribution to the oscillator strength from the in-plane continuum is negligible in the range of terahertz radiation of experimental interest [14, 15]. Thirdly, one can also regard the in-plane continuum as the source of the inhomogeneous broadening which was proposed by von Plessen and Thomas [16]. This inhomogeneous broadening may smear some characteristic peaks appearing in our present numerical simulations.

This TB approximation captures the qualitative features of real superlattices, and can give a fairly good description of their response within the strong-coupling regime [13]. It has been used with success by many groups [4, 11, 15, 17] in the past. For the Coulomb interaction we adopt the on-site model. In the absence of external electric fields, the contact Coulomb potential produces single bound states [15, 18]. In the dc–ac case, however, the situation changes significantly. For example, in the realm of the near-resonance case of Stark and ac-field frequencies, unequal spacing [19] between the Wannier–Stark ladders due to excitonic interaction can make the quasi-energy of the system present more than one bound Floquet state. The number of bound Floquet states is determined by how many distinct deviations there are between excitonic Wannier–Stark ladders and multiple ac-field quanta. This kind of Floquet bound state usually appears at low Wannier–Stark ladder indices. This case of more than one bound Floquet state has been discussed clearly and in great detail by Liu and Zhu, within the picture of dressed Wannier–Stark ladders [4, 15].

Because we assume that a *weak* ultrashort laser pulse excites the SL, instead of carrying out the perturbative expansion of semiconductor Bloch equations in terms of the order of $\mathcal{E}_0$, we take into account the full contributions from interband polarization. The nonlinear effect facilitated by the coupling of $n(k, t)$ with $p(k, t)$ on the lineshape of the fractional ladders will be discussed in the following. It is well known that the absorption coefficient can be expressed as

$$\alpha(\omega) \propto \mathrm{Im}\, \chi(\omega) = \mathrm{Im}[P(\omega)/\mathcal{E}(\omega)]$$

with $P(\omega)$ and $\mathcal{E}(\omega)$ being the Fourier transforms of $P(t) = \sum_k P_k(t)$ and $\mathcal{E}(t)$, respectively. We discuss separately two cases of interest, in which the ratio of the Stark frequency $\omega_B = eF_0d/\hbar$ to the THz-field frequency ω_{ac} is (i) an integer $\mathcal{N}$ and (ii) an irreducible fraction p/q.

Equations (1) and (2) were numerically integrated in the accelerated k-basis, where the drift term can be eliminated. Our results for the integer case $\omega_B = 2\omega_{ac} = 7\pi$ THz are shown in figure 1. Figure 1(a) is for the static case, while figure 1(b) is for $eF_1d/\hbar\omega_{ac} = 0.1$. The values of parameters used are: combined miniband width $\Delta = \Delta_c + \Delta_v = 40$ meV; Coulomb interaction strength $V = 10$ meV, comparable to the miniband width; dephasing rates

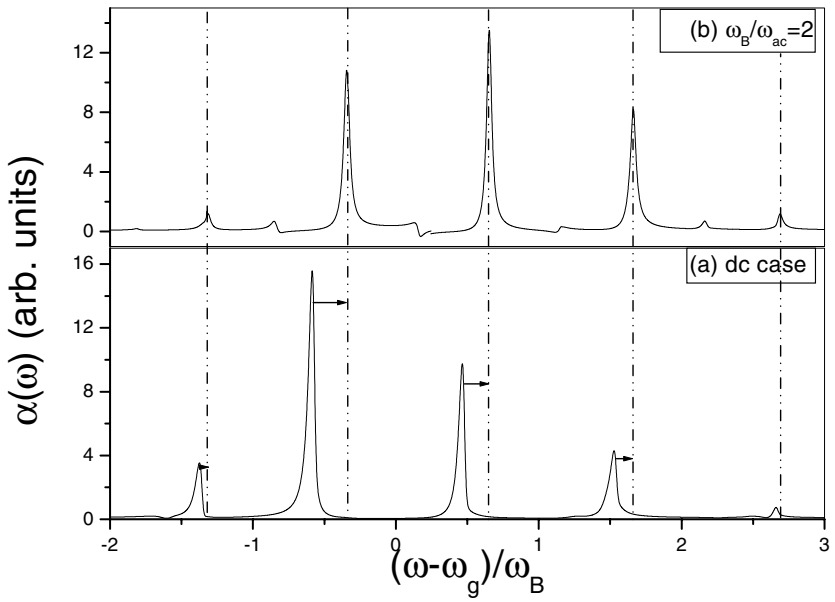

Figure 1. The spectrally resolved absorption coefficient $\alpha(\omega)$ for $\omega_B/\omega_{ac} = 2$ is plotted as a function of $\omega - \omega_g$ for two cases: (a) $edF_1/\hbar\omega_{ac} = 0.0$ (pure dc); (b) $edF_1/\hbar\omega_{ac} = 0.1$. The additional harmonics appear between neighbouring Stark resonances.

$\Gamma_T = \Gamma_L = 0.5$ THz; in the simulation of the coherent time evolution of the wave packets, the central frequency of the ultrashort laser pulse ω_L is tuned to be in resonance with the energy-gap frequency ω_g.

The Wannier–Stark resonances are clearly identified in figure 1(a). The frequency spacings are not equal, however, due to the excitonic interaction [19]. In figure 1(b) the spectrum appears more complex, showing a weak additional structure between any two main peaks. These weak structures exhibit either gain or absorption lineshapes, resulting from the nonlinear sum and difference frequency mixing of the dc and THz electric fields. It should be emphasized here that the ratio $edF_1/\hbar\omega_{ac}$ is a dominating factor in determining whether gain or absorption occurs. That is to say, changing the ratio $edF_1/\hbar\omega_{ac}$ may turn the resonance-type peaks into gain-type dips, or vice versa. The linewidth broadening of these structures also depends on the ratio $edF_1/\hbar\omega_{ac}$. This can be understood by noting that the quasi-energy band [20, 21] of a dc–ac-driven single-band TB system [22] is

$$\epsilon(k, \omega_{ac}) = E^{(0)} + \frac{\Delta}{2} J_n(edF_1/\hbar\omega_{ac}) \cos(kd)$$

with $\omega_B/\omega_{ac} = n$. According to the generalized golden rule in the single-particle picture, the rate of transition $P_{c\to v}(k)$ from the valence dressed band to the conduction dressed band, for every component k, is proportional to $\sum_n \delta[\epsilon_c(k, \omega_{ac}) - \epsilon_v(k, \omega_{ac}) + n\hbar\omega_{ac} - \hbar\omega_L]$ [23]. For every k, the transition can be viewed as a two-level system (TLS) with different energy spacing. These different energy spacings together with the *k-mixing* effect of the excitonic interaction lead to the broadening of the resonance peaks and gain dips. Of course, one can select the ratio $edF_1/\hbar\omega_{ac}$ to control the quasi-energy bandwidths and hence the broadening. Another feature, apparent when comparing figures 1(a) and 1(b), is the relative blue-shift of the *main* resonance peaks in the latter. These shifts are not equal, as emphasized by the horizontal arrows. Calculations were also made for other integer cases such as $\mathcal{N} = \omega_B/\omega_{ac} = 3, 4,$

yielding $\mathcal{N}$ resonance-type peaks or gain-type splittings in every Stark frequency interval ω_B. For reasons of space, they will not be discussed here.

Distinct asymmetric lineshapes of the peaks appear both in the dc-field and in the dc–ac-field field cases in figure 1. This asymmetry can be attributed to the Fano resonance [24]. The theoretical prediction of the Fano resonance in dc-biased semiconductor superlattices was made by Whittaker [25], Linder [19], Glutsch and Bechstedt [26], and was experimentally observed by Holfeld *et al* [27]. The mechanism of the Fano resonance is due to the coupling between the discrete and continuous excitonic states of the relative motion, mediated by the Coulomb interactions [19, 25–27]. The Fano resonances in dc–ac-driven (ω_B/ω an integer) superlattices were studied by Liu and Zhu [15]. The resonance takes effect through the coupling between the discrete *quasi-energy* excitons and sidebands of their continua.

The other interesting case is that where the ratio ω_B/ω_{ac} equals an irreducible fraction p/q. Figure 2 shows the spectrally resolved absorption coefficient for the cases $\omega_B/\omega_{ac} = 1/3$, $2/3$ and $4/3$. Here the same excitonic interaction strength and combined miniband width as in figure 1 are used. In all cases $edF_1/\hbar\omega_{ac} = 1.0$, and ω_{ac} is fixed at 7π THz.

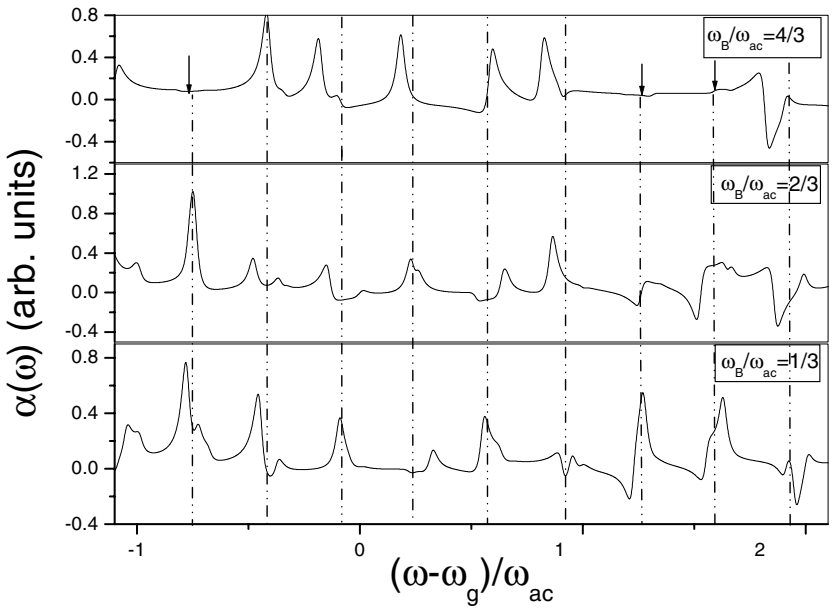

Figure 2. The spectrally resolved $\alpha(\omega)$ is plotted as a function of $\omega - \omega_g$ for the fractional cases $\omega_B/\omega_{ac} = 1/3, 2/3, 4/3$, showing the *excitonic* fractional ladders. The ratio $edF_1/\hbar\omega_{ac}$ is chosen to be 1.0, while the other parameters are the same as for figure 1.

Surprisingly, the resonances appear at approximately the same frequencies in all three panels, although the Stark frequencies in the top and bottom panels differ by a factor of four. In order to guide the eyes, dash–dot–dot vertical lines have been drawn through these resonances. It can also be seen from the figure that some resonances split into two peaks, which can be understood in the following context. The beating frequencies between the peaks in all panels are almost the same: $\frac{1}{3}\omega_{ac}$. This frequency equals neither the Stark frequency ω_B, which changes from panel to panel, nor the angular frequency of the ac field ω_{ac}. In fact, the quasi-energy band of the Hamiltonian driven by dc–ac electric fields with the ratio $\omega_B/\omega_{ac} = p/q$ is the underlying mechanism for the appearance of these peaks. Within the

one-electron and single-band approximations, these quasi-energy bands are given by

$$\epsilon_n(k) = A_q(k, \omega_B) + \frac{n}{p}\hbar\omega_B \qquad n = 0, 1, \ldots, p-1 \tag{3}$$

where $A_q(k, \omega_B)$ gives the band dispersion [8]. From the last term on the right-hand side of equation (3) it is evident that the quasi-energy band consists of p subbands with equal energy spacing $\hbar\omega_B/p$ ($\equiv\hbar\omega_{ac}/q$). The absorption spectrum reflects this energy gap through the generalized Fermi golden rule described above, while the term $A_q(k, \omega_B)$ is responsible for the broadening of the spectrum. The different values of ω_B/ω_{ac} taken in the three panels result in different values of $A_q(k, \omega_B)$ and, hence, different broadening. Also, the inclusion of the Coulomb interaction makes the positions of the peaks not exactly match the $\omega_{ac}/3$ rule. However, since on average there is one peak per $\omega_{ac}/3$ frequency interval, the structures are termed excitonic fractional ladders. Their *temporal* counterpart in the time-resolved four-wave-mixing spectrum has been discussed recently [17]. Results in the absence of excitonic interaction are presented in figure 3, where we used the same parameters as for figure 2 except that now $V = 0$. The fractional Stark ladder of spacing $\omega_{ac}/3$ can be clearly identified, with peaks distributed symmetrically about $\omega = \omega_g$, matching the $\omega_{ac}/3$ rule better than the excitonic case. These have been indicated by the vertical arrows in the upper panel of figure 2. Comparison of the fractional ladder lineshapes in figure 2 and figure 3 reveals that the purely Lorentzian lineshape of some peaks in figure 3 is absent for the corresponding peaks in figure 2, where the excitonic interaction is taken into account. This demonstrates that the excitonic interaction together with the Fano resonances destroys the symmetry and smears some resonance peaks. Here, the Fano interference with the small parameter q_f takes effect through the coupling of the discrete excitonic fractional ladders with the continuous sideband. It should be emphasized that the absorption signal depends also on the phase difference between the ultrashort laser pulse and the ac field. This important effect has been found recently by Meier *et al* [28] in an anisotropic 3D superlattice.

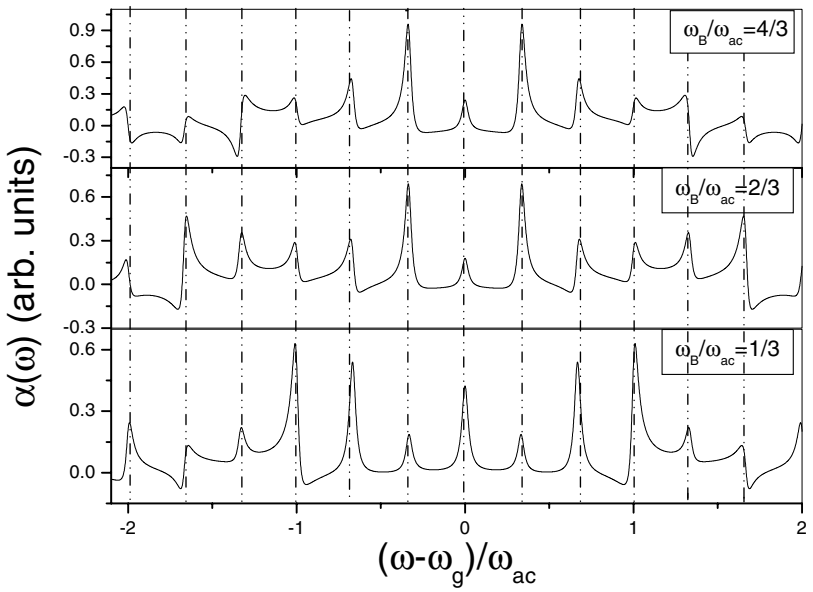

Figure 3. As figure 2, except that the excitonic interaction is absent. The fractional ladders are now symmetric about ω_g.

When the exciting laser field becomes strong, the nonlinear effect due to the high-order exciting laser-field magnitude $\mathcal{E}$ begins to take effect. The typical simulation of the effect is through the pump–probe configurations, where the weak probe laser field is delayed to time τ_p with respect to the strong pump field. Then the different linear and nonlinear signals can be extracted [29, 30]. This nonlinear effect makes the clear-cut fractional ladder harmonics broaden, tending to merge with each other. This is shown in figure 4, where the ratio of the exciting laser amplitude is indicated in the upper right corners of the respective panels. Here we only show the case of $\omega_B/\omega = 1/3$, and we use otherwise the same parameters as for figure 3, setting the time delay τ_p to 50 femtoseconds.

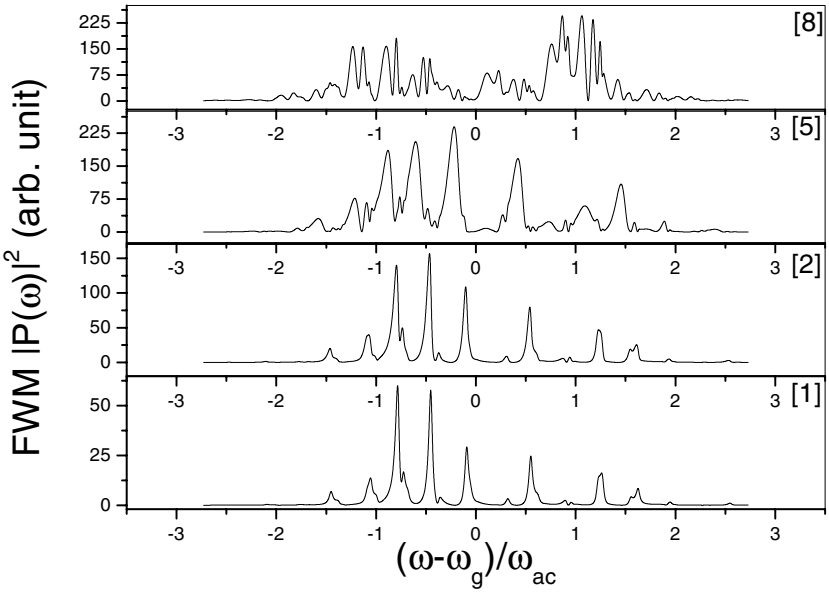

Figure 4. The pump–probe spectrally resolved four-wave-mixing signal squared $|P(\omega)|^2$ is shown in the four panels with the pump-field amplitude shown in the upper right corners (the amplitude of the pump-field in the lowest panel is assumed to be unity). Only the case of $\omega_B/\omega_{ac} = 1/3$ is shown; the other parameters used here are the same as for figure 2.

There is another interesting but subtle problem when the ratio ω_B/ω_{ac} is an irrational number. Numerical calculation cannot identify the essential difference between the rational and irrational cases. Physically, this difference will also be blurred by the scattering processes.

We now turn to the coherent dynamic evolution of electron–hole wave packets (WP). Results for a pure dc field have been previously reported by Dignam and co-workers, where Bloch oscillations were clearly demonstrated [14]. Meier *et al* studied relative motion in the exciton wavefunction in *momentum space* and found a dimensional crossover due to dynamic localization induced by a strong THz field [31, 32]. More recently Hughes and Citrin gave vivid pictures of the strongly anisotropic excitonic WP in optically excited semiconductor quantum wells driven by an in-plane THz field, through a time sequence of WP snapshots [33].

The WP coherent evolution may be described through the squared modulus of the real-space Fourier transform of the interband polarization

$$P(z,t) = \left| \sum_k \exp(-\mathrm{i}kz) P(k,t) \right|^2$$

giving the real-space description of the probability density of finding an electron and hole separated by z at time t [33]. It should be noted that wave packets cannot directly be probed by experiments, although it is theoretically interesting. In optically excited semiconductors, the centre-of-mass quasi-momentum of the electron–hole pair is always zero [3], which makes the description of the behaviour of the wave packets at the centre of mass difficult.

In order to elucidate the role the excitonic interaction plays in the profile of wave packets, we first present results in the absence of this interaction. Snapshots at various times are shown in figure 5, where the Stark and ac frequencies are chosen to have the same value 4π THz ($T_{ac} = 500$ fs), and $eF_1d/\hbar\omega_{ac}$ is set close to the first root of the first-order ordinary Bessel function (3.832).

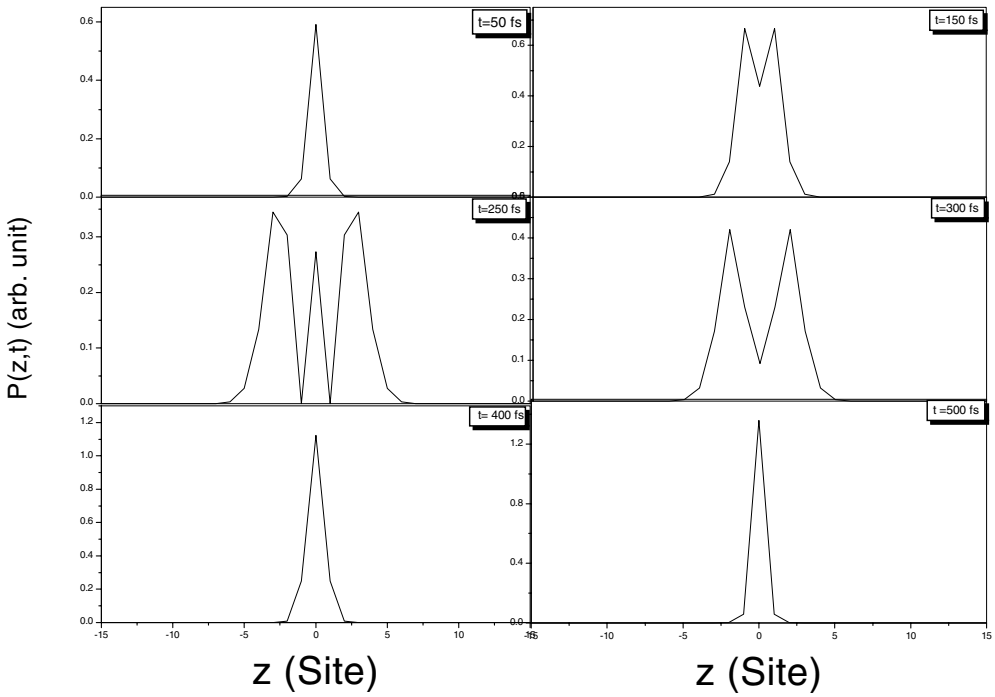

Figure 5. Coherent wave-packet evolution over time in the absence of excitonic interaction. The ratio $edF_1/\hbar\omega_{ac}$ is chosen to be 3.832, leading to dynamic localization within one cycle.

Note that at all times the WP is symmetric about the position $z = 0$. With the passage of time, it first splits into two parts and subsequently into three parts at half T_{ac}, when the size of the WP acquires its largest value within a cycle. After $T_{ac}/2$, the size begins to reduce. Due to the synchronous dynamic localization of electron and hole, at time $t = T_{ac}$, the size of the WP experiences the severe shrinkage shown in the last panel of figure 5. At later times, the WP will undergo the same expanding and shrinking processes in every time cycle (T_{ac}). This phenomenon demonstrates that dynamic localization has the ability to control the size of the WP. That is to say, that dynamic localization will make it impossible to find the electrons and holes simultaneously beyond a certain value of the relative coordinate. Also, comparison of figure 5 and figure 6 shows that dynamic localization makes the value of $P(z, t)$ larger at $z = 0$, demonstrating that it will enhance absorption. Figure 6 illustrates the same case as figure 5, except that we choose $eF_1d/\hbar\omega_{ac}$ to be 4.5. Now the WP also splits into three parts at time $t = T_{ac}/2$. The most important difference, however, is that now the size of the WP does *not*

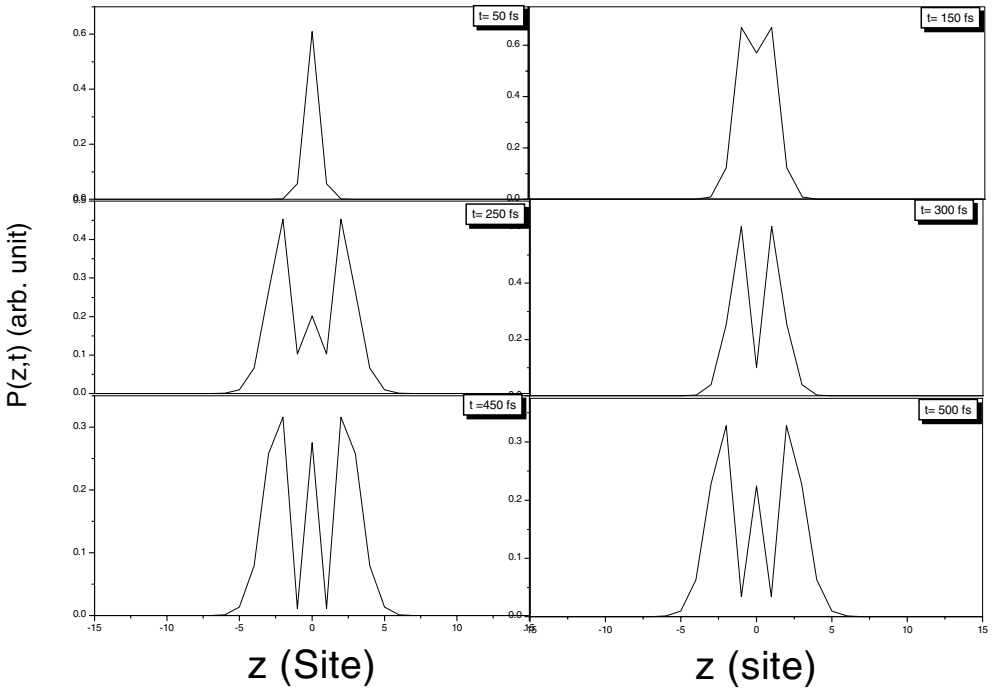

Figure 6. As figure 4, except that the ratio $edF_1/\hbar\omega_{ac}$ is chosen to be 4.50, leading to absence of dynamic localization.

experience shrinkage towards the end of the cycle. In fact, the size of the WP grows steadily with time, until it disappears due to dissipation. We next turn the excitonic interaction on, with the results showing a substantial change in the profile of the WP, as shown in figure 7. Here we use the same parameters as for figure 5. The WP becomes strongly anisotropic. Its height is reduced and although its extent still undergoes a shrinkage towards the end of the cycle, this shrinkage is less severe as compared with the noninteracting case. The splitting structure can be viewed as the spatial interference [33] induced by the Coulombic re-scattering due to the oscillating motion of the photo-generated electron–hole pair driven by dc–ac fields.

3. Conclusions

In summary, the spectrally resolved absorption and real-time wave packets of an optically excited semiconductor superlattice driven by combined parallel dc–ac electric fields are obtained by numerical integration of the semiconductor Bloch equations. The ratio of dc-field Stark frequency ω_B to ac-field frequency ω_{ac} determines the characteristic peaks of the absorption spectrum. When the ratio is a fraction, we identify for the first time the fractional ladders in the energy domain by taking into account the excitonic interaction, which we take as comparable to the miniband width. For the integer-$\mathcal{N}$ case we find $\mathcal{N}$ features within the frequency interval ω_B, corresponding to gain and resonant absorption. The effect of the dc–ac field on the size and profile of the WP shows that, as expected, dynamic localization vigorously curtails the elongation of the WP within one cycle, making its evolution behaviour that of a breathing mode. The excitonic interaction destroys the WP symmetry about its centre and softens the dynamic localization of the WP within one time cycle.

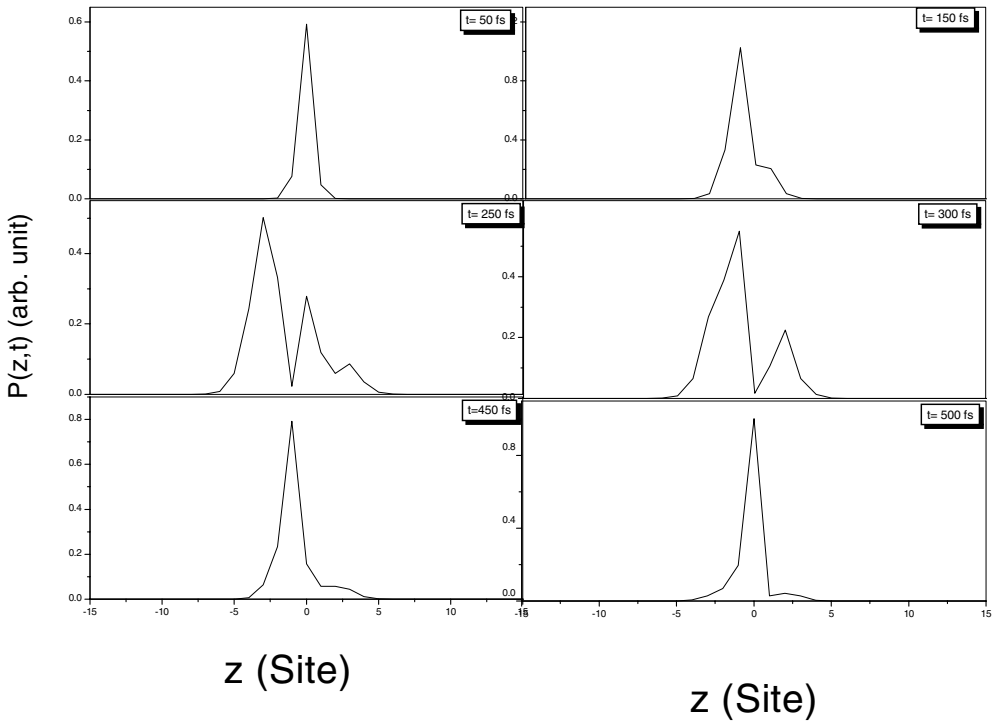

Figure 7. As figure 4, except that excitonic interaction is taken into account.

Acknowledgments

One of the authors (WY) is grateful for discussions with Professor Zdenka. This work was supported in part by Cátedra Presidencial en Ciencias (F.C.) and FONDECYT, Grants 1990425 and 3980014. WY is grateful for the generous hospitality of the Facultad de Fisica in PUC and Departmento de Fisica in UTFSM, where part of the work was done. WY is supported in part by the Youth Science Foundation of Shanxi Province of PRC, and also supported by CONICYT (3010052).

References

[1] Mendez E E and Bastard G 1993 *Phys. Today* **46** (6) 34
[2] Lyssenko V G, Valušis G, Löser F, Hasche T, Leo K, Dignam M M and Köhler K 1997 *Phys. Rev. Lett.* **79** 301
[3] Dignam M M 1999 *Phys. Rev.* B **59** 5770 and references therein
[4] Liu Ren-Bao and Zhu Bangfen 1999 *Phys. Rev.* B **59** 5759
[5] Unterrainer K, Keay B J, Wanke M C, Allen S J, Leonard D, Medeiros-Ribeiro G, Bhattacharya U and Rodwell M J W 1996 *Phys. Rev. Lett.* **76** 2973
[6] Kroemer H 2000 *Preprint* cond-mat/0007482
[7] Keay B J, Zeuner S, Allen S J, Maranowski K D, Gossard A C, Bhattacharya U and Rodwell M J W 1995 *Phys. Rev. Lett.* **75** 4102
[8] Zhao X-G, Jahnke R and Niu Q 1995 *Phys. Lett.* A **202** 297
[9] Madison K W, Fischer M C and Raizen M G 1999 *Phys. Rev.* A **60** R1767
[10] Haug H and Koch S W 1994 *Quantum Theory of the Optical and Electronic Properties of Semiconductors* 3rd edn (Singapore: World Scientific) and references therein
[11] Meier T, von Plessen G, Thomas P and Koch S W 1994 *Phys. Rev. Lett.* **73** 902

Meier T, von Plessen G, Thomas P and Koch S W 1995 *Phys. Rev.* B **51** 14 490
[12] Lindberg M and Koch S W 1988 *Phys. Rev.* B **38** 3342
[13] Silin A P 1985 *Sov. Phys.–USP* **28** 972
[14] Dignam M M, Sipe J E and Shah J 1994 *Phys. Rev.* B **49** 10 502
[15] Liu R-B and Zhu B-F 2000 *J. Phys.: Condens. Matter* **12** L741
[16] von Plessen G and Thomas P 1992 *Phys. Rev.* B **45** 9185
[17] Yan W, Zhao X-G and Wang H 1998 *J. Phys.: Condens. Matter* **10** L11
Yan W, Bao S-Q, Zhao X-G and Liang J Q 2000 *Phys. Rev.* B **61** 7269
[18] Egri I 1979 *Solid State Commun.* **32** 1017
Egri I 1982 *J. Phys. C: Solid State Phys.* **15** L461
[19] Linder N 1997 *Phys. Rev.* B **55** 13 664
[20] Holthaus M 1992 *Phys. Rev. Lett.* **69** 351
[21] Johnsen K and Jauho A-P 1999 *Phys. Rev. Lett.* **83** 1207
[22] Zak J 1993 *Phys. Rev. Lett.* **71** 2623
[23] Holthaus M 1992 *Z. Phys.* **89** 251
[24] Fano U *Phys. Rev.* **124** 1866
Glutsch S 1998 *Festkörperprobleme (Advances in Solid State Physics vol 37)* ed R Helbig (Braunschweig: Vieweg) p 151
The latter reference gives a recent review on the Fano resonance in semiconductors.
[25] Whittaker D M 1995 *Europhys. Lett.* **31** 55
[26] Glutsch S and Bechstedt F 1999 *Phys. Rev.* B **60** 16 584
[27] Holfeld C P, Löser F, Sudzius M, Leo K, Whittaker D M and Köhler K 1998 *Phys. Rev. Lett.* **81** 874
[28] Meier T, Kolbe H J, Thränhardt A, Weiser G, Thomas P and Koch S W 2000 *Physica* E **7** 267
[29] Lindberg M, Binder R and Koch S W 1992 *Phys. Rev.* A **45** 1865
[30] Bányai L, Tran Thoai D B, Reitsamer E, Haug H, Steinbach D, Wehner M U, Wegner M, Marschner T and Stolz W 1996 *Phys. Rev. Lett.* **75** 2188
[31] Dunlap D H and Kenkre V M 1986 *Phys. Rev.* B **34** 3625
[32] Meier T, Rossi F, Thomas P and Koch S W 1995 *Phys. Rev. Lett.* **75** 2558
[33] Hughes S and Citrin D S 1999 *Phys. Rev.* B **59** R5288